13:53:54 OCA PAD INITIATION - PROJECT HEADER INFORMATION 88

Active

Project #: G-41-683
Center # : R6525-0A0

Cost share #:
Center shr #:

Rev #: 0
OCA file #:
Work type : RES
Document : CONT
Contract entity: GTRC

Contract#: DAAL03-88-K-0154
Prime #:

Mod #:

Subprojects ? : N
Main project #:

Project unit: PHYSICS Unit code: 02.010.152
Project director(s):
GOLE J L PHYSICS

Sponsor/division names: ARMY / ARO, RES TRIANGLE PARK, NC
Sponsor/division codes: 102 / 001

Award period: 880701 to 881231 (performance) 890131 (reports)

Sponsor amount	New this change	Total to date
Contract value	20,000.00	20,000.00
Funded	20,000.00	20,000.00
Cost sharing amount		0.00

Does subcontracting plan apply ?: N

Title: CHEMICALLY DRIVEN VISIBLE LASER SYSTEMS

PROJECT ADMINISTRATION DATA

OCA contact: Ina R. Lashley 894-4820

Sponsor technical contact

DR DAVID SKATRUD, PHYSICS DIVISION
(000)000-0000
US ARMY RESEARCH OFFICE
P O BOX 12211
RESEARCH TRIANGLE PARK NC 72209-2211

Sponsor issuing office

MS PATSY S ASHE, CONTRACTING OFFICER
(919)549-0641
US ARMY RESEARCH OFFICE
P O BOX 12211
RESEARCH TRIANGLE PARK NC 72209-2211

Security class (U,C,S,TS) : U
Defense priority rating : NA
Equipment title vests with: Sponsor
NONE PROPOSED. (SEE BLOCK 27, CONT'D SHEET, RE PRIOR APPROVALS.)

ONR resident rep. is ACO (Y/N): Y
GOV'T supplemental sheet
GIT X

Administrative comments -
PROJECT INITIATION.

GEORGIA INSTITUTE OF TECHNOLOGY
OFFICE OF CONTRACT ADMINISTRATION

NOTICE OF PROJECT CLOSEOUT

Date 2/7/89

Project No. G-41-683 Center No. R6525-0A0

Project Director J.L. Gole School/Lab Physics

Sponsor ARMY

Contract/Grant No. DAAL03-88-K-0154 GTRC XX GIT ____

Prime Contract No. ____

Title Chemically Driven Visible Laser Systems

Effective Completion Date 12/31/88 (Performance) 1/31/89 (Reports)

Closeout Actions Required:

- ___ None
- X Final Invoice or Copy of Last Invoice
- X Final Report of Inventions and/or Subcontracts- Patent Questionnaire sent to P/
- X Government Property Inventory & Related Certificate
- ___ Classified Material Certificate
- X Release and Assignment
- ___ Other ____

Includes Subproject No(s). ____

Subproject Under Main Project No. ____

Continues Project No. ____ Continued by Project No. ____

Distribution:

- X Project Director
- X Administrative Network
- X Accounting
- X Procurement/GTRI Supply Services
- X Research Property Management
- ___ Research Security Services
- X Reports Coordinator (OCA)
- X GTRC
- X Project File
- X Contract Support Division (OCA) (2)
- ___ Other ____

G-41-623

Final Report

Chemically Pumped Visible Lasers

prepared for

Army Research Office

Short Term Innovative Research Program

by

James L. Gole

School of Physics

Georgia Institute of Technology

Atlanta, Georgia 30332

Under the auspices of the Short Term Innovative Research Program of the Army Research Office we have been engaged in the development of chemically pumped visible chemical laser ampliers and oscillators. This effort has now produced, the first visible chemical laser oscillator operative at 535 nm as well as indicated several additional promising systems. Our efforts have focused primarily on the generation of laser oscillation from an amplifying medium composed of thallium atoms in a temporarily creat4ed inverted population distribution. However we have also devoted some effort to the development of a gallium superfluorescent laser amplifier. We have made initial efforts to develop a lead atom (Pb) laser using an extrapolation of those concepts which have proven successful for the thallium and gallium systems. Further, we have carried out initial studies to investigate the potential for the creation of a CuCl gain medium. Here we have efficiently formed CuCl excited states with radiative lifetimes ranging to 60 microseconds!

We have employed certain unique aspects of a very select group of highly exothermic simple metal oxidations[1] and ultrafast energy transfer[2] in order to develop the first chemically driven superfluorescent laser amplifiers operative in the visible spectral region. These laser systems operate in a pulsed configuration (pulse width ~5nm FWHM) similar to a nitrogen laser and rely on ultrafast near resonant intermolecular energy transfer from metastable storage states formed in chemical reaction to subsequently lasing thallium (535nm) or gallium (417nm) atoms.[3]

To obtain superfluorescent laser pulses from efficiently pumped thallium atoms (see attached preprint[4]) we make use of near-resonant intermolecular energy transfer from metastable excited states of germanium monoxide, formed in the reaction of germanium atoms with ozone, and $X^2P_{1/2}$ ground state thallium atoms. This energy transfer rapidly populates the thallium $^2S_{1/2}$

excited state creating a population inversion with respect to the upper $X^2P_{3/2}$ component of the ground ^2P thallium atom configuration (Fig. 1). A system parameterization indicates that we have observed a superfluorescent laser pulse (Fig. 2) associated with the thallium 7 $^2S_{1/2}$ - 6 $^2P_{3/2}$ transition whose duration in a self-terminating system is ~5ns FWHM. The superfluorescent laser spike intensity is well in excess of ten times the normal $^2S_{1/2}$ - $^2P_{3/2}$ fluorescent intensity corresponding to a gain coefficient $\alpha \geq 2.3$ cm^{-1}. This superfluorescent lasing medium constituted by the thallium atom population inversion has now been employed in a full laser oscillator configuration (3% output coupling) with a subsequent ~10 fold increase in laser output power verses that obtained under single pass amplification and a corresponding increase in the ratio of superfluorescence to fluorescence ($I_{superfluorescence}/I_{fluorescence} \gtrsim 100$).

A similar albeit less pronounced superfluorescent laser spike can be generated from the more complex gallium system (Fig. 3) where both the initial thermal population of the Ga $^2P_{3/2}$ level (Fig. 4) and the possible reaction of both the $^2P_{3/2}$ and $^2P_{1/2}$ spin orbit components complicates a detailed analysis of the system. We find a gain coefficient, $\alpha \approx 2$ cm^{-1} for this superfluorescent laser amplifier. As the population of the $P_{3/2}$ metastable state builds to a sufficient level in the thallium and gallium system, the $^2S_{1/2}$ - $^2P_{3/2}$ population inversion is lost and lasing ceases. The light level in the remainder of the temporal scans depicted in Figs. 2 and 3 corresponds to $^2S_{1/2}$ - $^2P_{3/2}$ fluorescence.

Extension of the Tℓ, Ga Fast Near Resonant Intermolecular Energy Transfer Concept

Those studies focused on a pump of the thallium and gallium excited states X^* can be extended. The near resonant energy transfer concept can be

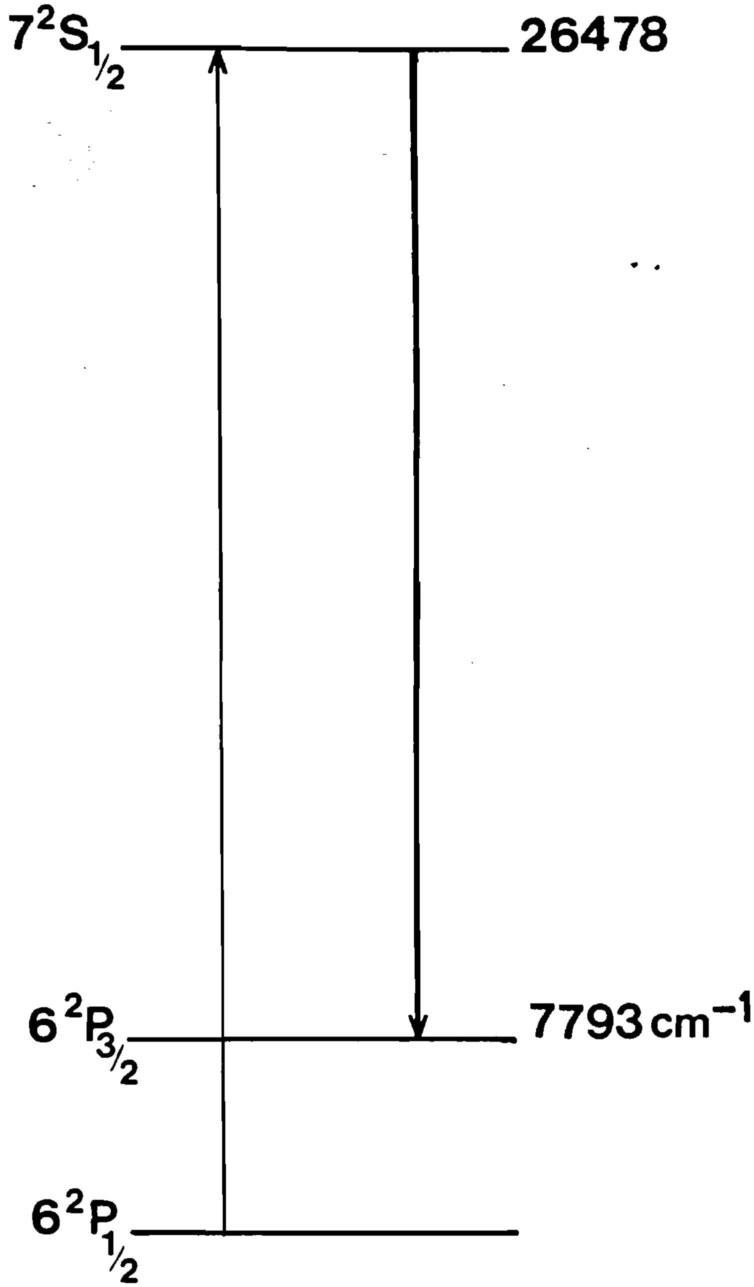

Figure 1

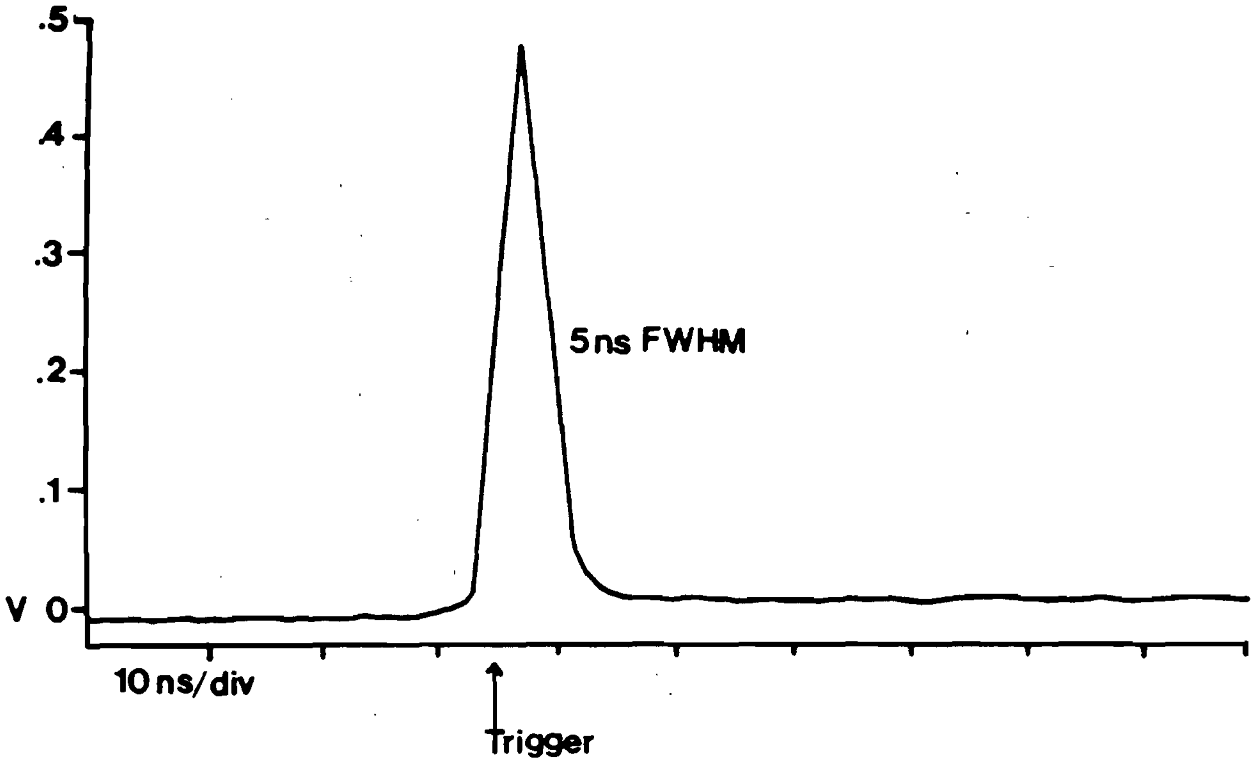

Figure 2

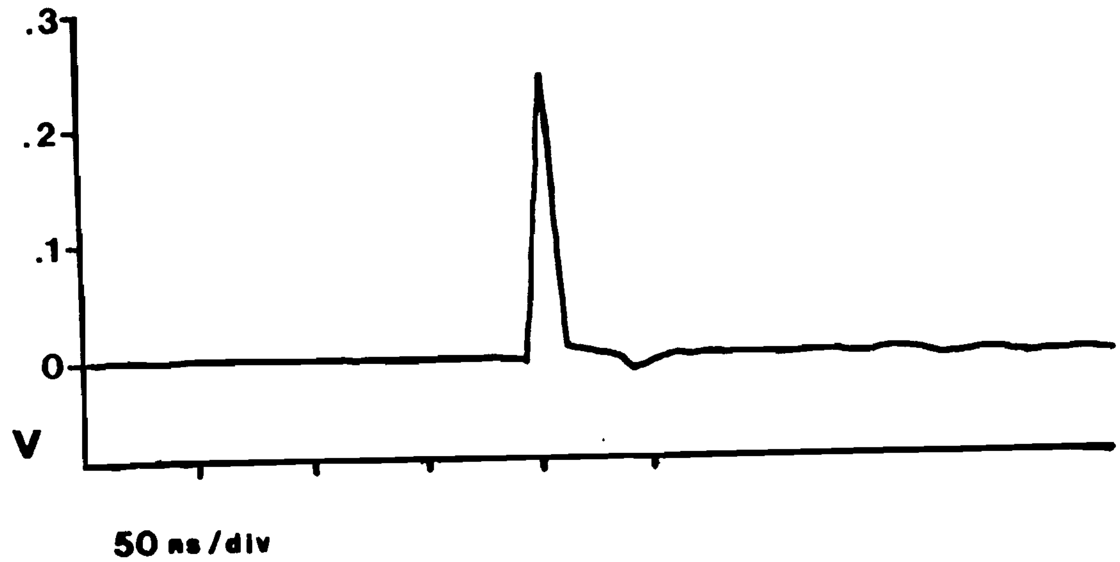

Figure 3

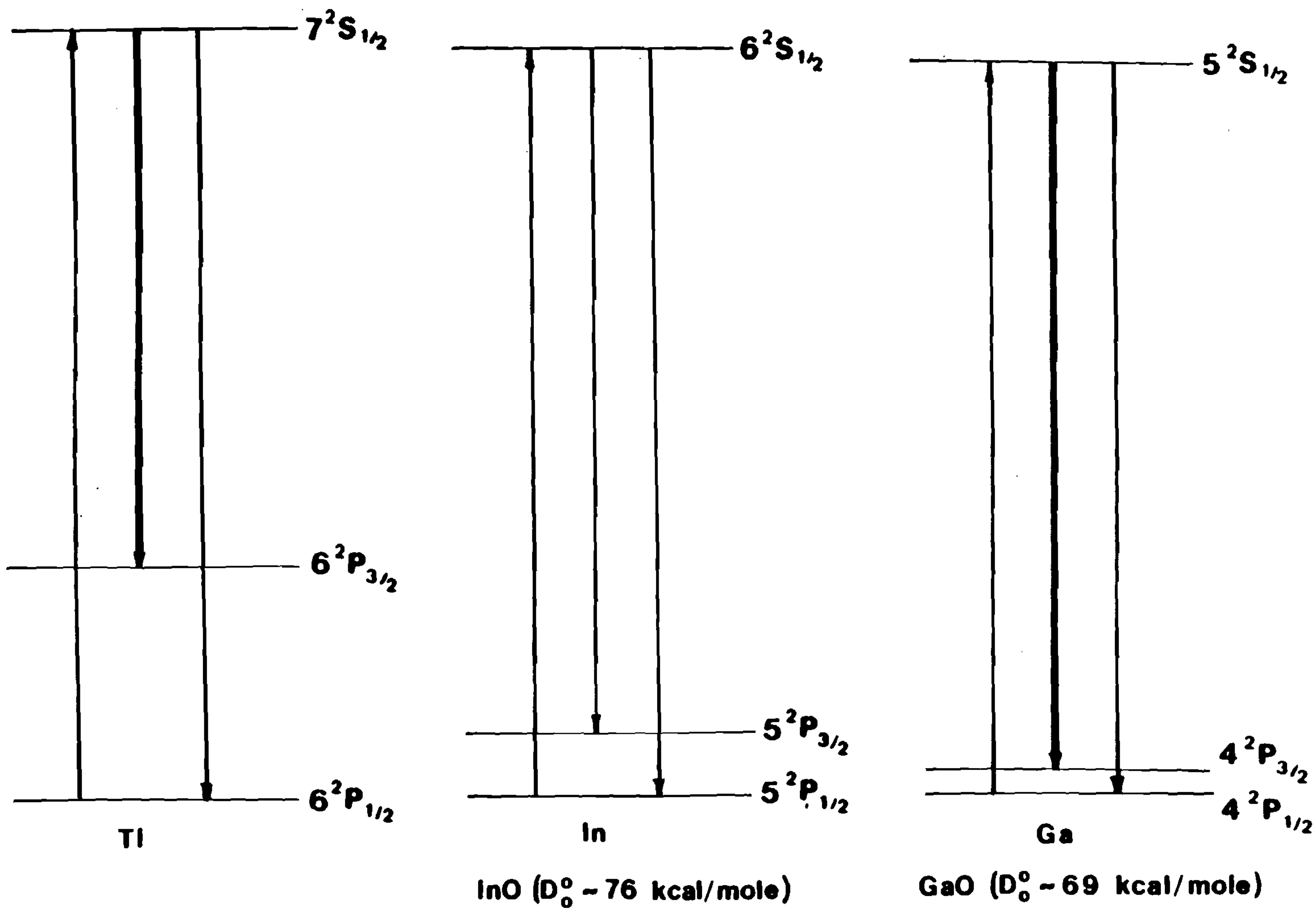
$7^2S_{1/2}$
$6^2P_{3/2}$
$6^2P_{1/2}$
Tl
$6^2S_{1/2}$
$5^2P_{3/2}$
$5^2P_{1/2}$
In
InO (D_o^o ~ 76 kcal/mole)
$5^2S_{1/2}$
$4^2P_{3/2}$
$4^2P_{1/2}$
Ga
GaO (D_o^o ~ 69 kcal/mole)

Figure 4

used as an efficient pump for somewhat longer lived emitters (allowing a further increase in energy storage in a laser cavity). Replacing the $X^2P_{3/2}$ spin orbit component with a different spin-orbit level or a low-lying electronic state in a variety of atomic receptors, we generalize the near resonant intermolecular energy transfer pump-amplification concept to a broader range of possible lasing configurations.

As applied to energy transfer involving Tℓ, Ga, and In atoms, the results which we have obtained thusfar indicate (1) the importance of the near matchup of SiO and GeO energy level increments with the energy level spacing of the receptor atoms of interest and (2) the potential for operation over a rather wide range of intermediate ($P_{3/2}$) and ground state ($P_{1/2}$) level separations. With the extension to low-lying electronic states, the three level excitation scheme (Ex: Figure 1) offers a considerable range of radiative configurations (lifetimes) commensurate with a variety of potential lasing transitions.

Making use of a few evaluated and several inferable radiative lifetimes, we have successfully identified a number of three level schemes where, in large part, an energy transfer pump from the metastable states of SiO and GeO can be accomplished with a near resonant intermolecular energy transfer to a potentially lasing atomic receptor state whose radiative lifetime varies from several nanoseconds to several microseconds, the transitions within themselves covering a range of visible wavelengths. Further, within this pumping scheme, lasing occurs to a state which is either weakly or strongly coupled to the ground state, this combination providing a range of pump-amplifier schemes. Most of the systems considered offer the possibility of pump transitions which are closer in resonance to SiO and GeO than are the energy levels of the Group III atoms, Ga, Tℓ, and In. Thus they are potentially more efficient.

The first of these systems which we are pursuing involves a pump amplification configuration in direct analogy to the thallium and gallium systems. Particularly, we focus on the pumping of several strongly or weakly optically coupled transitions in lead where we again make use of the large spin orgit splittings (Fig. 5) characterizing the ground electronic ^3P states of this atom. We are attempting to employ near resonant energy transfer from SiO and GeO metastable states to pump the $^3P_0$ component of the ground electronic state of the lead atom.[5]

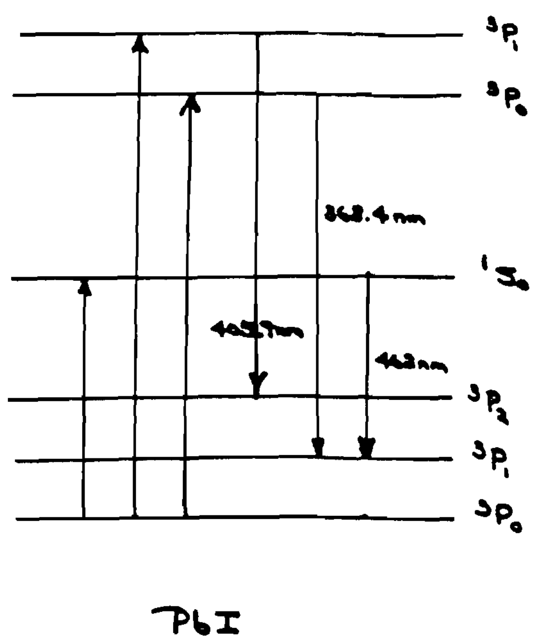

Figure 5

The pump transitions indicated are in closer resonance to SiO and GeO metastable level separations than are the energy levels of the Group III atoms Ga, Tℓ, and In. Thus the energy transfer pump should be inherently considerably more efficient.

Initial experiments involving the lead system focused on an attempt to pump the transitions of interest using metastable GeO generated in the germanium-ozone reaction. The envisioned Ge-O_3-Pb→GeO^*-Pb-GeO-Pb^* system is not successful because lead competes effectively with germanium for the available O_3 and the reactive branching is dominated by PbO^* formation. This initial result suggests an alternate configuration which involves the reaction of silicon atoms with NO_2 to form the metastable states of SiO, these metastable states subsequently transferring their stored energy to the lead atom. The Pb-NO_2 reaction is not sufficiently exothermic to produce excited state lead oxide products. Further, there is reason to believe that the very exothermic Si-NO_2 reaction may compete effectively with the mildly exothermic Pb-NO_2 reaction even though coulombic forces are expected to play a greater role in the latter process. Initial studies of the Si-NO_2-Pb system are currently beginning in our laboratory.

We have also carried out some preliminary work involving the study of highly efficient processes forming the surprisingly long-lived low-lying electronic states of the copper chloride molecule (CuCℓ). The data in Figure 6 demonstrate (1) a strongly pressure dependent emission process associated with electronically excited $CuC\ell^*$ formation across the pressure range from near single collision to multiple collision conditions, (2) significant emission associated especially with the very long-lived CuCℓ $A^3\Pi_2$-$X^1\Sigma$ band system, and (3) the manifestation of ultrafast energy transfer among strongly coupled CuCℓ excited states. The reaction sequence

$$Cu(^2D) + C\ell_2 \rightarrow CuC\ell^* + C\ell$$

$$CuC\ell^* + M \rightarrow CuC\ell^{*'} + M \qquad \text{(collisional relaxation)}$$

$$CuC\ell^* \rightarrow CuC\ell^t + h\nu$$

$$CuC\ell^{*'} \rightarrow CuC\ell^{t'} + h\nu$$

is appropriate to describe the reaction of electronically excited $Cu(^2D)$ atoms and the formation and deactivation processes associated with $CuC\ell^*$ formation and emission. As Table 1 taken from Delaval et al.[6] demonstrates,

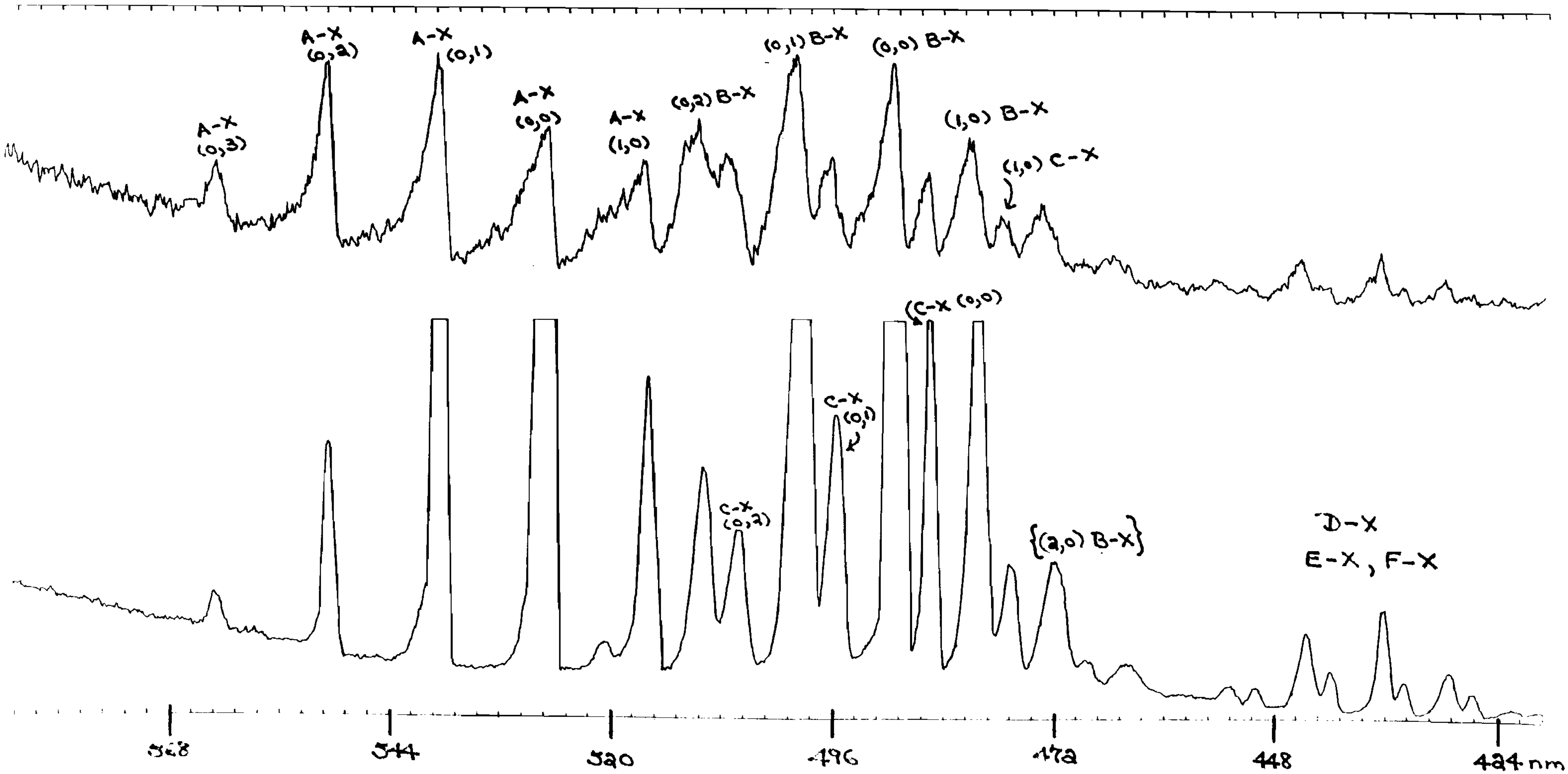
A-X (0,3)
A-X (0,2)
A-X (0,1)
A-X (0,0)
A-X (1,0)
(0,2) B-X
(0,1) B-X
(0,0) B-X
(1,0) B-X
(1,0) C-X
C-X (0,0)
C-X (0,1)
C-X (0,2)
(2,0) B-X
D-X
E-X, F-X
568
544
520
496
472
448
424 nm

Figure 6

Table 1

Excited Electronic State	Excitation wavelength (Å)	Observation wavelength (Å)	Lifetime[a] (μs)
F $^3\Delta_1$ (v=0)	4022	3956	6.3
E $^1\Sigma$ (v=0)	4333	4333	0.43
D $^1\Pi$ (v=0)	4354	4354	0.45
C $^3\Pi_0$ (v=0)	4847	4847	3.2
B $^3\Pi_1$ (v=0)	4881	4881	3.3
A $^3\Pi_2$ (v=0)	5271	5271	60

[a]Relative error can be evaluated to ± 10%.

the radiative lifetimes associated with six low-lying states of CuCℓ are all reasonably long-lived reaching a maximum of 60 microseconds for A $^3\Pi_2$, v=0. The observed chemiluminescent emission intensities associated with excited state CuCℓ emission in the sequence above belie the long lifetimes associated with these CuCℓ excited states. Further, a even longer-lived lower-lying $a^3\Sigma^+$ state[7] is likely also populated in the above reaction sequence. The v = 11 and v = 12 levels of this $a^3\Sigma^+$ state are virtually isoergic with the v' = 0 and v' = 1 levels of A $^3\Pi_2$. There is evidence of fast near resonant intramolecular energy transfer between the $a^3\Sigma^+$ and A $^3\Pi_2$ states associated with these levels.

We believe that the features associated with the A-X emission system at ~518, ~528, ~540, and ~552 nm may form the basis for laser systems at one or more of these wavelengths. Based upon our recent studies of amplifier formation in the Na_3-X (Cℓ,Br,I) system[8] we envision the above sequence followed by

$$CuC\ell^{t \text{ or } t'} + C\ell_2 \rightarrow CuC\ell_2$$

to remove the terminal laser level. We hope to pursue this study further in the near future.

References

1. "Energy Balance and Branching Ratios Associated with the Chemiluminescent Reaction $Si(^3P) + N_2O(^1\Sigma) \rightarrow SiO^*(a^3\Sigma^+, b^3\Pi, A^1\Pi) + N_2(v''\geq 5)$ - Possible Formation of Vibrationally Excited N_2 in $M + N_2O$ Reactions," with G. J. Green, Chemical Physics 100, 133 (1985).

   "Energy Balance in the $Si\text{-}NO_2$ Reaction: On the Formation of SiO $a^3\Sigma^+$, $v' \geq 0$, and Ultrafast $a^3\Sigma^+ - b^3\Pi$ E-E Energy Transfer," Chemical Physics 100, 153 (1985).
2. "Probing Ultrafast Energy Transfer Among the Excited States of Small High Temperature Molecules," in "Gas Phase Chemiluminescence and Chemi-ionization," A. Fontijn (editor) - Elsevier Science Publishers, 1985, p. 253.
3. "Superfluorescent Chemically Driven Laser Transitions Using Fast Near Resonant Energy Transfer," with J. R. Woodward and S. H. Cobb, Proceedings of the Fourth International Laser Science Conference, in press.
4. K. K. Shen, J. R. Woodward, S. H. Cobb, and J. L. Gole, "A Chemically Driven Visible Laser Operative at 535nm," submitted for publication.
5. C. E. Moore, "Atomic Energy Levels," N. B. S. Circular 467, Volume III.
6. J. M. Delaval, Y. Lefebvre, H. Bocquet, P. Bernage, and P. Niay, Chemical Physics 111, 129 (1987).
7. P. R. Rao and P. R. Rao, Spectry. Letters 7, 463 (1974).
8. "A Chemical Process Producing a Continuous Laser Amplifier in the Visible Region," with S. H. Cobb and R. Woodward, Chem. Phys. Lett. 143, 205 (1988).

"Continuous Chemical Amplification of Single and Multimode Lasers in the Visible Region," with S. H. Cobb and J. R. Woodward, Chemical Physics Letters, in press.

"Continuous Chemical Laser Amplifiers in the Visible Region," with S. H. Cobb and J. R. Woodward, Proceedings of the Fourth International Laser Science Conference, in press.

A Chemically Driven Visible Laser Operative At 535nm.

K. K. Shen, J. R. Woodward,* S. H. Cobb,† and James L. Gole

High Temperature Laboratory

Center for Atomic and Molecular Science

and

School of Physics

Georgia Institute of Technology

Atlanta, Georgia 30332

†Present address, Dept. of Physics, Murray State University.

*Present address, Lamp Division, The General Electric Company, Cleveland, Ohio

Abstract

The first purely chemical visible laser system based on an efficient near resonant energy transfer from metastable excited triplet states of germanium monoxide, formed in the reaction of germanium atoms with ozone, and $X^2P_{1/2}$ ground state thallium atoms is reported. This energy transfer rapidly populates the thallium $^2S_{1/2}$ excited state creating a temporary population inversion with respect to the upper $X^2P_{3/2}$ component of the ground ^2P thallium atom configuration. A system parameterization indicates the observation of a superfluorescent laser pulse created on the thallium $7\ ^2S_{1/2} - 6\ ^2P_{3/2}$ transition whose duration in a self-terminating system is ~5ns FWHM. This single pass superfluorescent system is converted to a multipass laser oscillator (3% output coupling) with a corresponding increase in laser output power correlating with a substantial increase in the ratio of superfluorescence to fluorescence and the display of a significant directionality. This approach, which makes use of fast intermolecular energy transfer, shows the promise of extrapolation to several additional systems.

Introduction

The development of chemically driven visible lasers has attracted the attention of several researchers over the past twenty years. It has been suggested that most successful electronic transition chemical lasers will require a two step approach in which chemical energy is released and stored in a first step and this energy is then transferred to an appropriate laser medium in a second step.[1] We have implemented this approach to obtain visible chemical laser action in the form of a superfluorescent laser pulse and subsequent laser oscillation associated with the thallium 7 $^2S_{1/2}$ - 6 $^2P_{3/2}$ transition where the thallium 7 $^2S_{1/2}$ level is chemically pumped through energy transfer from the low-lying metastable a $^3\Sigma^+$ and $b^3\Pi$ states of SiO and GeO, the products of a highly exothermic metal oxidation.[2]

We employ the near resonant fast intermolecular transfer scheme[2]

$$\text{Pump:}\quad MO^* + X^2P_{1/2} \rightarrow X^* \, (^2S_{1/2}) + MO^t \tag{1}$$

$$\text{Lasing:}\quad X^* \, (^2S_{1/2}) \rightarrow X \, (^2P_{3/2}) + h\nu \tag{2}$$

where the metal oxide excitation is transferred to the thallium atom whence it is pumped from the ground X $^2P_{1/2}$ state to the energetically accessible electronically excited $^2S_{1/2}$ level. Subsequently thallium atoms in the $^2S_{1/2}$ level emit radiation via the $^2S_{1/2}$ - $X^2P_{3/2}$ transition, to the upper $^2P_{3/2}$ spin orbit component of the ground electronic state with which they have formed a temporary population inversion. This transition has now been used to demonstrate superfluorescent lasing action and oscillation.

The success of the outlined approach depends on (1) our ability to produce copious quantities of the SiO and GeO metastable energy storage states in "high quantum yield" chemiluminescent reactions,[2] (2) our ability to produce sufficient thallium atom $X^2P_{1/2}$ concentrations and simultaneously minimal $X^2P_{3/2}$ concentrations before the processes (1) and (2) are made to occur,[2] and (3) near resonant (highly efficient) intermolecular energy transfers (Figure 1) that can take place between the SiO and GeO metastable states and those levels accessible via excitation of the lowest $^2P_{1/2}$ spin orbit component of the thallium atom.

Given that the requisite concentrations are obtained, the upper $^2P_{3/2}$ component of the ground state thallium atom can act as the terminal level in a three level laser provided that this state is not populated before the lasing pump-sequence (1,2) is initiated. Thallium was chosen for initial experiments because its X $^2P_{3/2}$ level is 7793 cm^{-1}[3] above the X $^2P_{1/2}$ level thus preventing thermal excitation of this level ($N_{3/2} \leq 10^{-10}$ ($N_{1/2}$) at $T \leq 1100K$) during vaporization, subsequent entrainment, and passage to the reaction zone, and insuring its population exclusively through the reaction sequence (1,2). Thallium is also an ideal candidate because it will not compete with those reactive processes forming the metastable states of SiO and GeO. The $T\ell O$ bond is weak if not unstable,[4] any oxidation processes producing it being highly endothermic.

Experimental - Initial Parameterization

Experimental apparatus designs and procedures for the oxidation of Si and Ge have been explained in detail elsewhere.[2] Here, we focus on the Ge-O_3 metathesis and the Ge-O_3-GeO^*-$T\ell$ system. Briefly, germanium was held in a carbon crucible heated by a tungsten basket heater (Fig. 2(a) - R. D. Mathis). The metal was heated to temperatures in excess of 1800K corresponding to a metal vapor pressure in the range 10^{-1} to 1 Torr to produce a near effusive vapor further drawn out of the oven region by an entraining argon flow, forming a flux in the reaction zone well in excess of 10^{17} atom/cm^2-sec. An entrained Ge flux will react with N_2O under multiple collision conditions to produce the a $^3\Sigma^+$ state of GeO and with O_3 to produce the $a^3\Sigma^+$, $b^3\Pi$, and $A^1\Pi$ states of GeO, where triplet state formation dominates this latter reactive branching.

Thallium was placed in an aluminum oxide crucible and heated again with a tungsten basket heater to temperatures ranging to 1100K (Fig. 2(a)). The typical maximum operating temperature provides approximately a 1 Torr vapor pressure in steady flow; the effects of a cooler entraining argon stream were reduced by heating the argon inlet tube with a Ta wire resistive heater. Argon carrier gas was passed into connecting alumina tubes and through the top of the thallium crucible, forming a flow of $T\ell$/Ar directed perpendicular to and intersecting the reaction zone (Figure 2(a)). The $T\ell$ flux to this zone ranges from $\sim 5\times10^{18}/cm^2$-sec to $\sim 8\times10^{20}/cm^2$-sec.

The necessary oxidant was introduced into the reaction zone via a concentric ring injector system (Figure 2(a)). The effect of X $^2P_{1/2}$ atoms on the GeO triplet state fluorescence was studied in order to demonstrate efficient energy transfer from GeO to $T\ell$. Here the thallium was introduced into a clearly visible GeO flame producing a bright green fluorescence. However, in those experiments in which the temporal behavior of the $T\ell$ ($^2S_{1/2}$) fluorescence or superfluorescence was monitored, the $T\ell$ and Ge atoms were first intimately mixed and then the reactive and energy transfer sequences were initiated through the introduction of ozone. The entire reaction zone configuration was placed in a considerably larger vacuum chamber (Fig. 2(a),(b)) which facilitated a sharp dropoff in reactant concentrations away from the reactant mixing region.

Energy Transfer - Concentration Levels and Self-Absorption

Initial experiments[5] which monitored GeO^* and $T\ell^*$ emission focused on the observation of the GeO^* - $T\ell$ energy transfer and demonstrated a very efficient process. The manifestation of this energy transfer was readily observed with the thallium oven system operative at temperatures ranging from $\sim$800K, corresponding to a thallium vapor pressure of 10^{-2} Torr. A clear symbiotic relation could be established between the depletion of the GeO^* $a^3\Sigma^+$ and $b^3\Pi$

emissions and the subsequent enhancement of $T\ell$ 7 ^2S-6 ^2P emission spectra. Systematic elimination of the reactants involved in the metal oxidation considered demonstrated that the formation of the GeO^* metastable species was required to observe the atomic fluorescence from thallium.[5]

At thallium pressures of 10^{-2} Torr ($T\ell$ conc. in rxn. zone $\sim 10^{14}$/cc), the ratio of $T\ell$ $^2S_{1/2}$-$^2P_{3/2}$ (535nm) to $T\ell$ $^2S_{1/2}$-$^2P_{1/2}$ (377.6nm) fluorescence is in virtual agreement with the oscillator strength ratio $A_{535}/A_{377.6} = 1.16 \pm 0.06$.[6] At thallium pressures close to 1 Torr ($[T\ell] \sim 10^{16}$/cc), evidence is obtained for $^2P_{1/2}$ self absorption as the intensities of the $^2S_{1/2}$-$^2P_{3/2}$ and $^2S_{1/2}$ - $^2P_{1/2}$ fluorescence features are in the ratio of $\sim$ 8:1.[5] However, it can readily be demonstrated that the concentration of $P_{3/2}$ atoms produced in the reaction sequence (1,2) is far below that required for self absorption.[5] At the highest $T\ell$ ^{2}concentations, the pumping scheme outlined previously and considered in more detail shortly will produce approximately 2 x 10^{11} $^2P_{3/2}$ $T\ell$ atoms/cc in the reaction zone over the period in which lasing action is observed. This concentration is some three orders of magnitude less than that producing no apparent self absorption due to $T\ell$ $^2P_{1/2}$.

<u>Observation of Superfluorescence</u>

The thallium $6^2P_{3/2}$ level is metastable, the $6^2P_{3/2}$-$6^2P_{1/2}$ ($X^2P_{3/2}$-$X^2P_{1/2}$) radiative lifetime being between 0.1 and 1 second.[7] Thus, the $^2P_{3/2}$ state atoms must be removed from the mixing and reaction zone either through diffusion or collisional deactivation (see following) or lasing action will cease. A laser operating on the $7^2S_{1/2}$-$6^2P_{3/2}$ transition will be self terminating. In analogy to the nitrogen laser, the observation of amplified spontaneous emission or superfluorescence preceding a fluorescence component and at a much greater intensity signals the creation of a temporary population inversion and the observation of a stimulated emission process.

We have employed a Spex 1704 - RCA 4840 PMT combination in conjunction with fast temporal monitoring of the emission signal from the $^2S_{1/2}$-$^2P_{3/2}$ Tℓ transition to assess this occurrance. The spectrometer was set at 535.1nm to overlap the $^2S_{1/2}$-$^2P_{3/2}$ Tℓ emission feature and the photomultiplier output was sent to a LeCroy 9400 125 MHz digital oscilloscope and recorded on a Hewlett-Packard plotter. We have made use of the Ge-O_3 reaction, the onset of metal oxide formation and the subsequent energy transfer sequence being controlled with the O_3 flow through a triggered pulsed valve or a manual needle valve. With the Ge and Tℓ flows into the reaction zone established (Tℓ $\sim 9\times10^{15}$ atoms/cc, Ge $> 2\times10^{12}$ atoms/cc), the O_3 was introduced into the reaction zone, initiating GeO^* metastable formation and energy transfer to the Tℓ atoms, with laser emission subsequently detected.

In order to detect superfluorescence, the digital oscilloscope was triggered by the laser emission at a level set higher than the signal from the Tℓ fluorescence or the dark current from the PMT. The observed fluorescence signal from the thallium 535.1nm line was measured at approximately 50 mV while the time resolved superfluorescence was measured at approximately ten times this level with a FWHM of $\sim$ 5 ns (Figures 3(a), 3(b)). It is important to emphasize that the trigger indicated in Fig. 3(b) does not correspond to the introduction of O_3 into the system but rather to a flag of the laser emission level. Further, the 30ns time frame does not correspond to the reactant mixing time. We monitor the system after reaction and energy transfer have been initiated and the laser emission corresponding to the $^2S_{1/2}$ - $^2P_{3/2}$ transition builds to a triggering level. When the Spex monochromator was set so as to monitor Tℓ fluorescence features at 377.7 (Tℓ $7^2S_{1/2}$ - $6^2P_{1/2}$) and 352.5nm (Tℓ ^2D - $6^2P_{3/2}$) or an MO^* emission feature, no signal spike (Figure 3(b)) attributable to superfluorescence was observed.

A further intriguing aspect of the GeO^{*} - $T\ell$ system which indicates the system duty cycle is represented in Figure 3(c). It is possible to observe repeating superfluorescent spikes while monitoring the 535.1nm, $7^2S_{1/2}$-$6^2P_{3/2}$ $T\ell$ fluorescence. These spikes result from experimental instabilities which occasionally reduce the supply of one of the three components required to produce $T\ell$ $^2S_{1/2}$ and halt the $T\ell$ fluorescence for $t \geq 10\mu s$, allowing the subsequent recycling of the superfluorescence. That is, if the energy transfer event is interrupted long enough so as to produce a complete loss of the fluorescence signal for $t \geq 10\mu s$, the $6^2P_{3/2}$ state of thallium is depleted to the extent that when the energy transfer sequence is resumed, the population inversion between the $7^2S_{1/2}$ and $6^2P_{3/2}$ levels is again temporarily established. An absence of the fluorescence for $t \geq 10\mu s$ can result from the loss of any of the reactants from the reaction zone. The $6^2P_{3/2}$ level population may be depleted through diffusion out of the reaction-energy transfer zone and away from the photon path to the detector employed in the experiment or through relaxation to the $6^2P_{1/2}$ level.[5]

Laser Oscillation

In order to convert superfluorescent laser amplification into laser oscillation, a full cavity configuration was constructed as in Fig. 2(c) with two Brewster angle windows (Mellos Griot BK-7 (n=1.519)) optimized at 535nm to minimize reflectivity losses. The optical cavity consists of two concave mirrors, one totally reflective mirror whose radius of curvature is 2m and an output coupler of 3% transmissivity also with 2m radius of curvature. The cavity length is 30 cm (reaction zone 1-1.5cm) and thus the two mirrors are in a stable resonator configuration. A HeNe laser which is used to align the cavity also specifies the region of the much shorter reaction zone which will be sampled. Note that the "lever arm" formed by the HeNe laser beam about the reaction zone as it passes through this region central to the 30 cm cavity has a significant moment as the present system by no means constitutes an optimal cavity configuration. The large lever arm also complicates cavity alignment.

This laser system was also probed temporally using the 125 MHz digital oscilloscope in conjunction with two configurations. In the first, the laser cavity was aligned with the incident slit of a Spex 1704 monochromator set at 535.1nm, operating at 1nm resolution, and placed ~20 cm behind the output coupling mirror of the laser cavity. The output from the RCA 4840 PMT used previously to monitor superfluorescence was again sent to the digital oscilloscope. The signal recorded in full cavity configuration (Fig. 4(a)) is approximately a factor of ten more intense than the superfluorescent laser pulse recorded in the absence of a full laser cavity and focusing lens (Figs. 2(b),(c)). Further, the superfluorescence to fluorescence ratio increases to well over 100.

In a second experimental configuration, we replaced the spectrometer with a fast photodiode (LeCroix Model 40D Optical Detector - risetime $<$ 1.0ns) placed 20cm from the laser cavity. The output from this photodiode (Fig. 4(b)) was again sent directly to the digital oscilloscope. The signal level recorded was approximately three times that from a 1mW HeNe laser impinging directly onto the photodiode and placed 2cm away. The multiple peaks observed in the photodiode scan of the laser cavity result from the diffusion of a substantial thallium atom concentration through the reaction zone and a subsequent pump-oscillation sequence at different positions within the reaction zone.

In both of the experiments described, when the laser cavity mirrors are walked from their aligned positions, lasing action can be made to cease and no signals are detected. We suggest that the combination of results obtained in the present study demonstrates the temporal and directional characteristics which are to be associated with the first visible chemical laser.

Discussion - Future Considerations

A consideration of our experimental configuration and reactant concentrations leads us to believe that the laser emission which we observe is superfluorescence as opposed to amplified spontaneous emission. Based upon the geometry of the system and the visual observation of the thallium fluorescence, we assume a cylindrical amplification zone of length 1 cm and diameter 1/4 cm, with a $^2S_{1/2}$ - $^2P_{3/2}$ population difference which corresponds initially to a concentration $\Delta N = 2\times10^{11}/cm^3$.[8] Our estimated reaction length, $\mathcal{L}$ = 1-2cm is much shorter than the cooperation length, $\mathcal{L}_c$ = 35 cm, calculated from the relation

$$\mathcal{L}_c = \phi\ (4\pi c\ \tau_{sp}/(\Delta N)\lambda^2)^{1/2}$$

where $\phi = \ln\ (2\pi/\theta_o) = 16$ ($\theta_o = (\Delta N)^{-1/2}\ (2\pi)^{-1/4}\ (\alpha L)^{-3/4} \simeq 6\times10^{-7}$, α = gain coefficient) is a logarithmic function of θ_o, the initial tipping angle of the Bloch vector. The gain coefficient, $\alpha = 2.3\ cm^{-1}$, is determined on the basis of $G = e^{\alpha\mathcal{L}} = 10$ for one pass through the reaction zone, τ_{sp} is the $^2S_{1/2}$ radiative lifetime = 7.5×10^{-9}s, and λ = 535.1 nm is the wavelength of the transition.

An $\mathcal{L}_c$ much greater than $\mathcal{L}$ indicates that it is reasonable to conclude that the laser emission corresponds to superfluorescence.[9] Amplified spontaneous emission (nitrogen laser), in contrast, requires that $\mathcal{L}$ be much greater than $\mathcal{L}_c$.[10] For an initially totally inverted superfluorescent system, ϕ typically has a value between 10 and 25 in agreement with our determined value. Based upon our observed gain, G = 10, and our estimated reaction length of 1 cm, we determine a gain coefficient, $\alpha = 2.3\ cm^{-1}$. This coefficient can also be calculated from the relation

$$\alpha = (T_2/\tau_{sp})(\Delta N)\lambda^2/8\pi = 3.3\ cm^{-1}$$

where $T_2 = 1.1\times10^{-9}$ sec is the reciprocal of the inhomogeneous Doppler linewidth and all other quantities have been defined previously. It is to be noted that the α value determined in these experiments represents a lower bound due primarily to the response time of the digital oscilloscope. If we attempt to correct for this response time, the superfluorescence/fluorescence ratio may be as much as 2.5 times greater than detected. This would correspond to an α value of 3.2 cm^{-1}. The agreement between the determined values of α is quite encouraging.

Finally, the temporal width of the superfluorescence output pulse can be calculated from the relation

$$\tau_w = \phi\,(8\pi\tau_{sp}/(\Delta N)\lambda^2 \ell)$$

to be 5.3×10^{-9} sec. This value should be compared to our measured FWHM of ~ 5×10^{-9} sec (Fig. 3(b)).

The extension of these experiments to the remaining Group IIIA atoms, gallium and indium is complicated by (1) the reactivity of the gallium and indium atoms to those oxidants used to produce the metastable states of SiO and GeO and (2) the smaller spin orbit splittings of the gallium and indium X^2P levels leading to the thermal population of the $X^2P_{3/2}$ level. Nevertheless, superfluorescence associated with the gallium $^2S_{1/2}$-$^2P_{3/2}$ transition has been detected at 417nm. These experiments will be discussed in a future publication.[5]

Acknowledgement

It is a pleasure to acknowledge most helpful discussions with Drs. R. C. Oldenborg and S. Baughcum concerning this study. The support of the Army Research Office through the Short Term Innovative Research Program at the right time is most appreciated.

References

1. Short Wavelength Chemical Laser Workshop, Charleston, S.C., Nov. 14-15, 1984.

2. J. L. Gole and G. J. Green, Chemical Physics 100, 133 (1985), R. Woodward, J. S. Hayden, and J. L. Gole, Chemical Physics 100, 153 (1985) and references therein.

3. C. E. Moore, Atomic Energy Levels, Vol. 3, Natl. Stand. Ref. Data Series, Natl. Bur. Stand. 35 (1971).

4. H. G. Howell, Proc. Phys. Soc. 57, 32 (1945).

5. Chemically Driven Visible Laser Transitions and Oscillation Using Fast Near Resonant Energy Transfer to Group IIIA Metals", S. H. Cobb, J. R. Woodward, K. K. Shen, and J. L. Gole, in preparation.

6. A. Gallagher and A. Lurio, Phys. Rev. 136, A87 (1964).

7. J. Wiesenfeld, private communication.

8. Determined on the basis of (1) the estimated concentration of GeO^* produced in the reaction zone and (2) the assumption of a gas kinetic rate for the transfer of the energy stored in GeO^* to the thallium atom to produce $T\ell^*$ ($^2S_{1/2}$). The Ge concentration in the reaction zone ranges between 0.7 and 2×10^{13} atom/cc whereas the ozone concentration is between 1 and 7×10^{14}/cc. Using the rate constant of Davis et al. for the Si-N_2O reaction (8.11×10^{-11} cm^3/atom-sec- P. M. Swearengen, S. J. Davis, and T. M. Niemczyk, Chem. Phys. Lett. 55, 274 (1978)), and assuming a quantum yield of 10%, we find the rate of GeO^* production is ~ 5×10^{16} sec^{-1}. With a thallium atom concentration ~ 9×10^{15}/cc and a gas kinetic rate constant for the energy transfer from GeO^* to $T\ell$, we estimate the $T\ell^*$ formation rate as 2×10^{19} sec^{-1} in the reaction zone leading to a buildup of the $T\ell$ $^2S_{1/2}$ state to the 10^{11}/cc range in approximately 10 ns.

9. J. C. MacGilliuray and M. S. Feld, Phys. Rev. A23, 1334 (1981).

10. O. Suelto, in Principles of Lasers, 2nd Edition, (Plenum Press, 1982).

Figure Captions

Figure 1: Energy level diagrams for thallium, SiO a-x, and GeO a-x indicating the energy matchup between various a-x energy increments associated with v' = 0 and the thallium electronic level structure.

Figure 2: (a) Oven configurations and orientations for (1) the vaporization of thallium subsequently entrained in argon in a horizontal gas flow and (2) germanium entrained in argon and subsequently oxidized with O_3 to produce the metastable $a^3\Sigma^+$ and $b^3\Pi$ states of GeO (and the much shorter lived $A^1\Pi$ state.

(b) Overview of oven systems and photon path to the spectrometer/ PMT detection system for single pass amplification studies. The 1 cm x .25 cm reaction zone was estimated by visual observation of the Tℓ fluorescence. The circle indicates the Ge oven system and the oxidant ring inlet.

(c) Overview of full laser cavity configuration showing aligning HeNe laser and positions of photodiode and spectrometer - PMT detectors.

Figure 3: (a) Tℓ 7 $^2S_{1/2}$ - 6 $^2P_{3/2}$ (535.1nm) fluorescence pumped through energy transfer from GeO^* ($a^3\Sigma^+$,$b^3\Pi$) formed in the Ge-O_3 reaction. As the O_3 source valve opens, the Tℓ fluorescence signal reaches its maximum; with the O_3 valve closed the Tℓ fluorescence slowly diminishes. Superfluorescence is not detected because of the temporal resolution of the oscilloscope associated with this long time scale.

(b) Tℓ 7 $^2S_{1/2}$ - 6 $^2P_{3/2}$ (535.1nm) superfluorescence observed at a signal trigger level of 0.2V. The trigger of the superfluorescence is by signal level and not by reactant mixing which occurs on a much longer time scale. The measured FWHM is ~ 5 nsec compared to $\tau \sim 7.5$ n-sec, the radiative lifetime of the $7\ ^2S_{1/2}$ level. A return to the fluorescence level is seen subsequent to the superfluorescent pulse.

(c) $T\ell\ 7\ ^2S_{1/2} - 6\ ^2P_{3/2}$ (535.1nm) fluorescence + superfluorescence in a system suffering an interruption of the reaction-energy transfer process. In the region (B) we observe a thallium superfluorescence signal following an $\sim 10\mu s$ absence of the thallium fluorescence. In the region (C) we return to the $T\ell$ fluorescence signal level following the self termination of the superfluorescence due to population of the $T\ell\ 6\ ^2P_{3/2}$ level.

Figure 4: (a) $T\ell\ 7\ ^2S_{1/2} - 6\ ^2P_{3/2}$ (535.1nm) superfluorescent oscillation observed with full laser cavity configuration. The ratio of the superfluorescence to that fluorescence which follows after self termination of lasing action and is barely visible in the figure is close to 100.

(b) Photodiode digital oscilloscope signal detected from laser cavity with a fast photodiode positioned 20cm from the output coupling mirror (3% transmittance) of the cavity. The multiple peaks are ascribed to multiple oscillation regions throughout the $Ge\text{-}O_3\text{-}T\ell \rightarrow GeO^*\text{-}T\ell \rightarrow GeO\text{-}T\ell^*$ reaction zone.

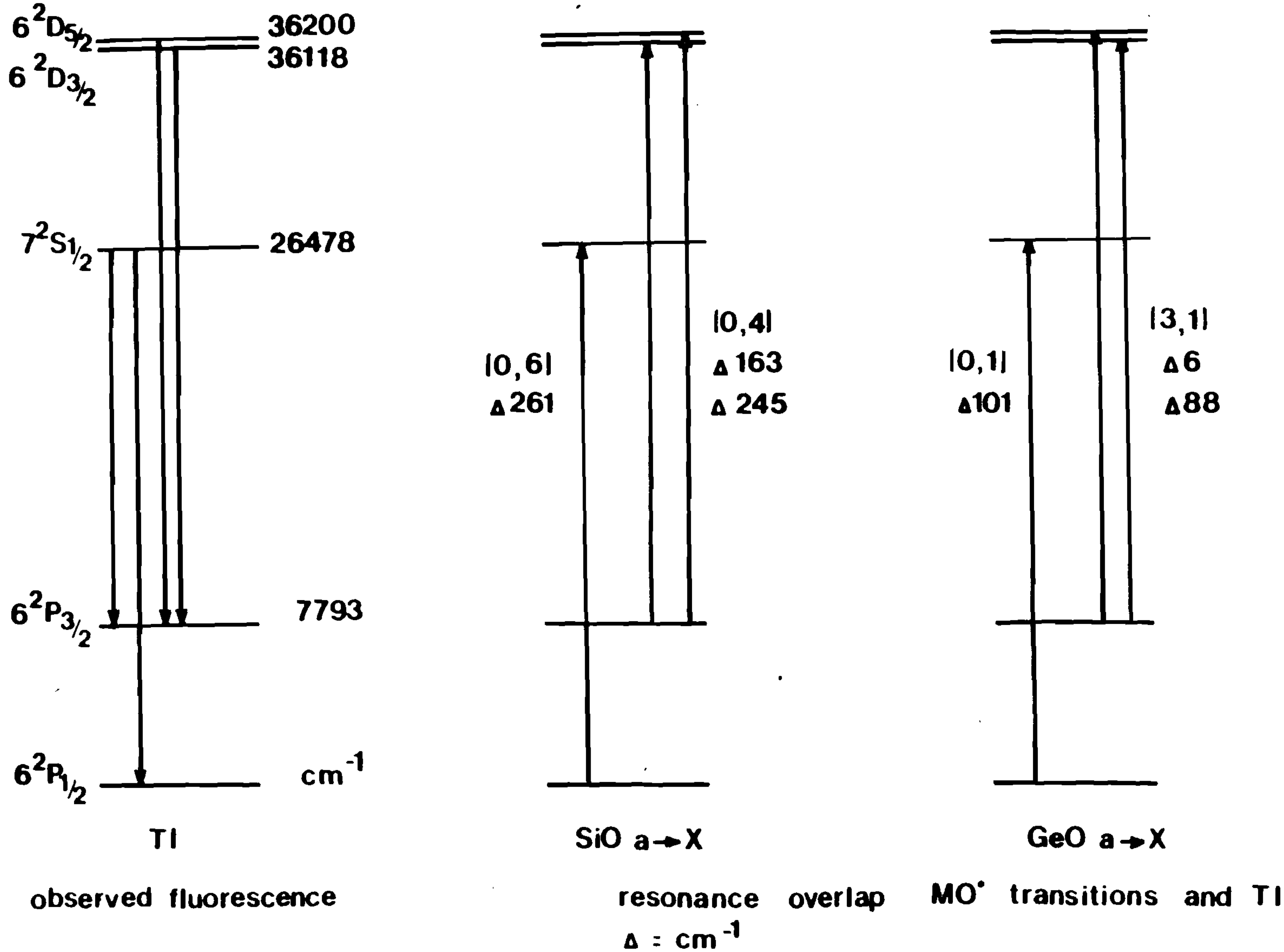
$6^2D_{5/2}$
$6^2D_{3/2}$
36200
36118
$7^2S_{1/2}$
26478
$6^2P_{3/2}$
7793
$6^2P_{1/2}$
cm^{-1}
|0,6|
Δ261
|0,4|
Δ163
Δ245
|0,1|
Δ101
|3,1|
Δ6
Δ88
Tl
SiO a→X
GeO a→X
observed fluorescence
resonance overlap MO* transitions and Tl
Δ : cm^{-1}

Figure 1

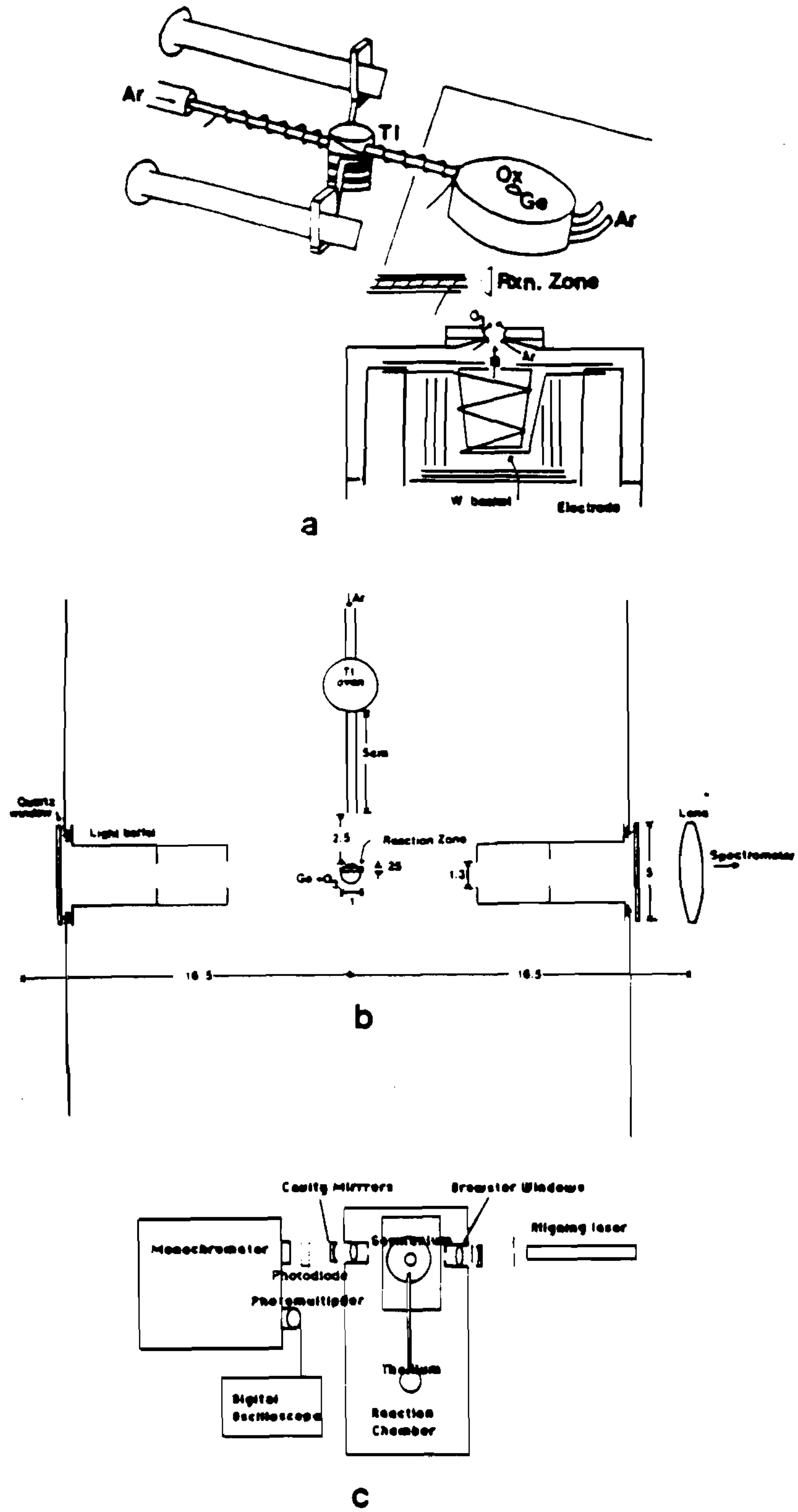
Ar
Tl
Ox
Ge
Ar
Rxn. Zone
W basket
Electrode
a
Ar
Reaction Zone
2.5
1.3
5
Lens
Spectrometer
16.5
16.5
b
Cavity Mirrors
Brewster Windows
Aligning laser
Monochromator
Photodiode
Photomultiplier
Digital Oscilloscope
Thallium
Reaction Chamber
c

Figure 2

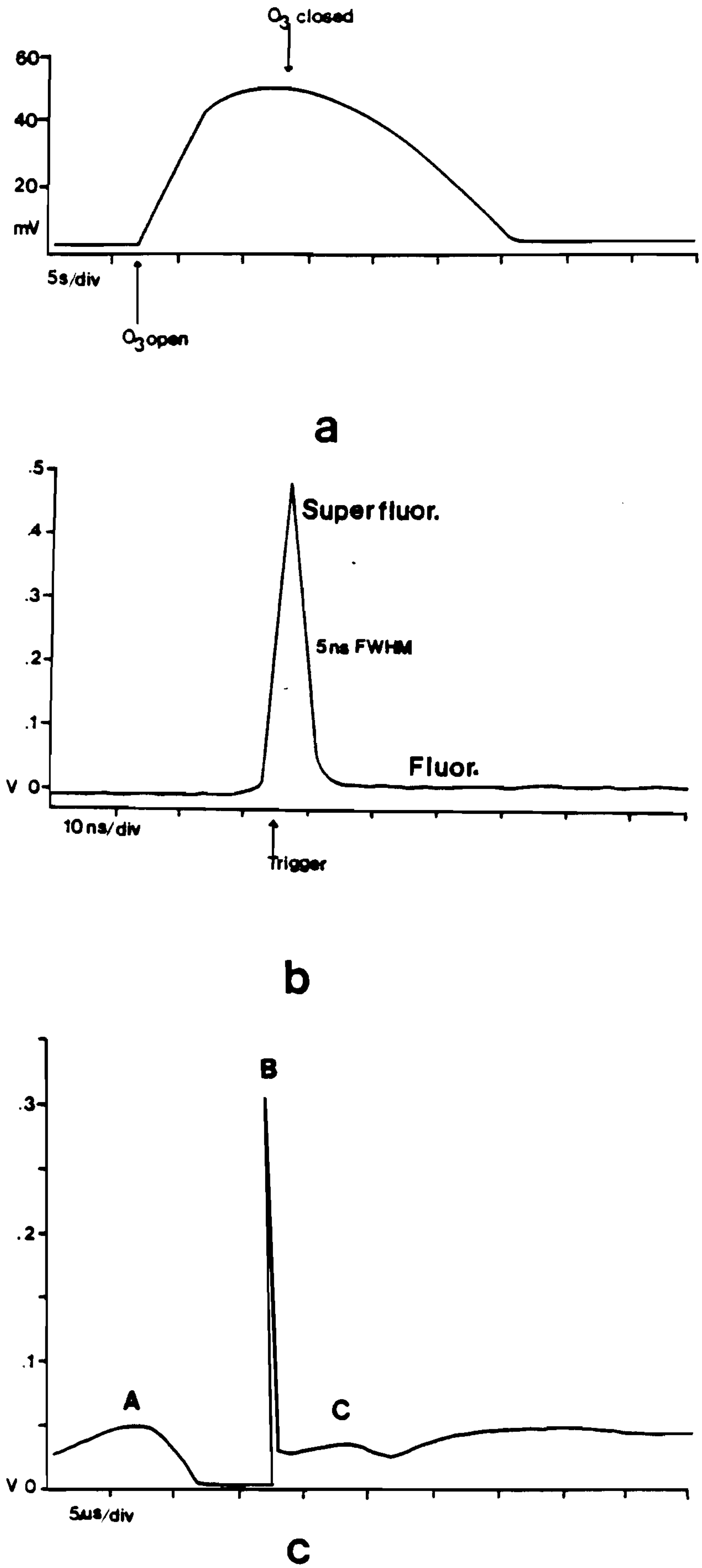
O3 closed
60
40
20
mV
5s/div
O3 open
a
.5
.4
.3
.2
.1
V 0
Superfluor.
5ns FWHM
Fluor.
10 ns/div
Trigger
b
.3
.2
.1
V 0
B
A
C
5μs/div
c

Figure 3

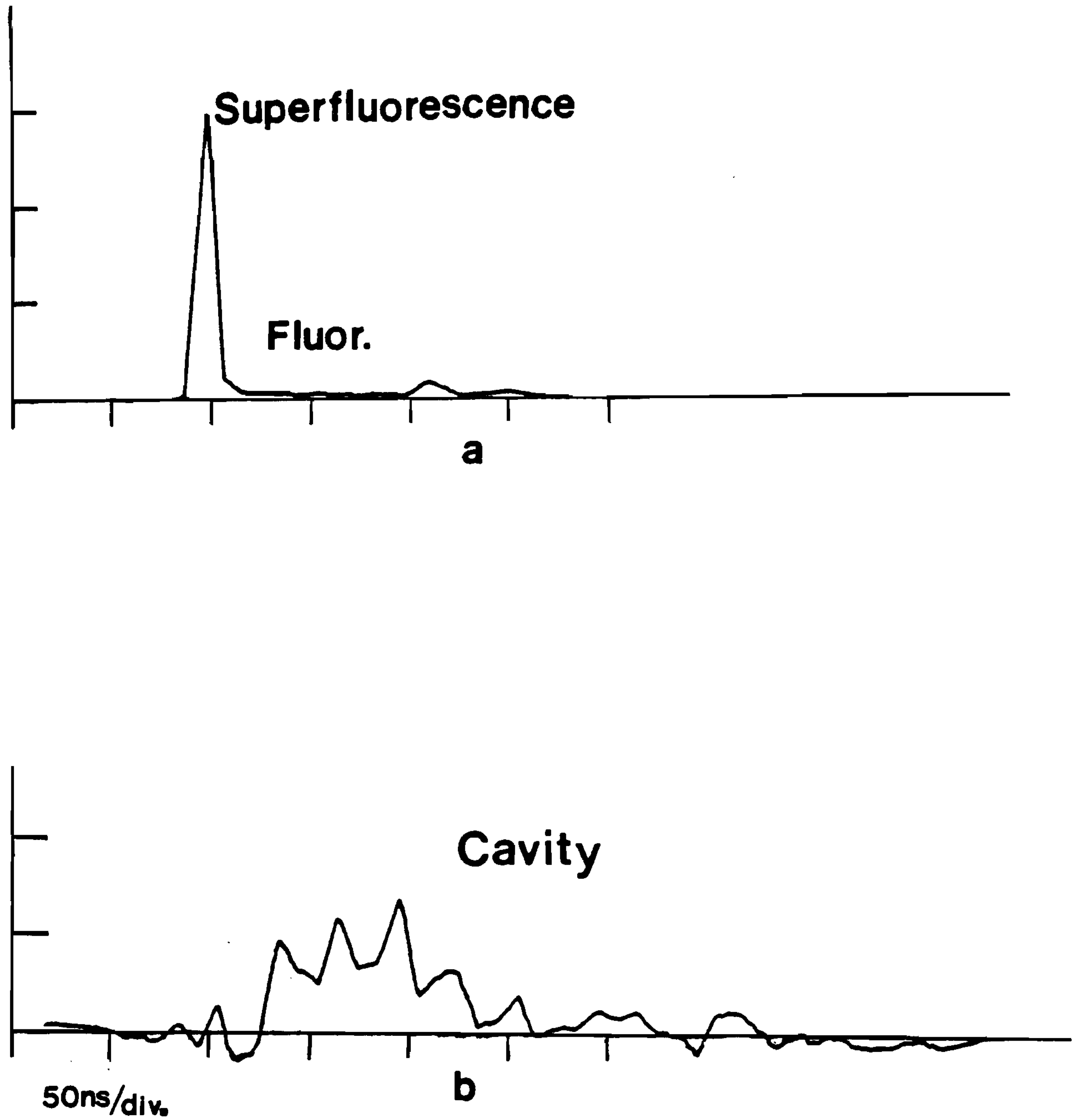

Figure 4